

Multibeam Two-Plasmon Decay in Three Dimensions: Thresholds and Saturation

The parametric resonance of oscillators or waves is an effect that exists in areas of physics as diverse as geophysical fluid dynamics and galactic dynamics. Instabilities caused by the parametric excitation of waves in plasmas resulting from the presence of large-amplitude electromagnetic waves are of immediate concern to inertial confinement fusion (ICF),^{1,2} high-energy-density physics (HEDP),³ and ionospheric modification experiments.⁴ Most theoretical and numerical works to date have assumed that instability is driven by a single electromagnetic (EM) pump wave, despite the fact that almost all ICF and HEDP experiments overlap many beams. How instability is modified when multiple pump waves are present is an issue of practical and theoretical interest. Recent indirect-drive experiments at the National Ignition Facility (NIF) (where 96 beams overlap near each of the two laser entrance holes of a plasma-filled hohlraum) are examples that highlight the importance of cooperative, multibeam parametric instability. In these experiments a multibeam parametric instability known as cross-beam energy transfer (CBET) was shown to have a dramatic effect on implosion symmetry and target performance.^{5,6} In direct-drive ICF, where the fusion target is directly irradiated by many overlapping laser beams, two-plasmon decay (TPD) can occur. This problem has been studied for 40+ years, but there has been a strong resurgence of interest because of ignition-scale experiments on the NIF. TPD is important because it can generate hot electrons, which represent a preheat risk to the target.⁷ TPD is a three-wave decay instability in which an EM wave of frequency ω_0 and wave vector \vec{k}_0 decays into two electrostatic Langmuir waves (LW's), satisfying the resonance conditions $\omega_0 = \omega + \omega'$ and $\vec{k}_0 = \vec{k} + \vec{k}'$, where ω , ω' , and \vec{k} , \vec{k}' are the frequencies and wave vectors of the decay LW's, respectively. This instability can occur in the coronal plasma at electron densities close to the quarter-critical density $n_c/4$, where $n_c [= m_e \omega_0^2 / (4\pi e^2)]$ is the electron density at which EM waves are reflected. Here, e and m_e are the electron charge and mass, respectively.

In this article we present a linear three-dimensional (3-D) numerical stability analysis of TPD in an inhomogeneous plasma driven by multiple laser beams. This is followed by an investigation of the subsequent nonlinear evolution, where non-

linearity enters by the coupling of the LW's to low-frequency density perturbations. This model was in part motivated by a favorable comparison of the results with more-detailed, fully kinetic calculations in regimes where they can be compared (i.e., in two spatial dimensions).⁸ The existence of two forms of cooperative multibeam TPD instability is demonstrated. One form shares short-wavelength, high-group-velocity, collective (or common) LW's that convectively saturate (i.e., the waves undergo a finite spatial amplification),⁶ while the other is associated with shared long-wavelength, small-group-velocity LW's and is absolutely unstable (i.e., the waves grow in time). The identification of an absolutely unstable collective mode of instability is a new discovery. Furthermore, it is shown to have the lowest threshold in most cases. The presence of absolute instability with a low threshold renders the TPD an inherently nonlinear problem.

The linear stability of multibeam TPD can be investigated by solving a linearized equation for the envelope of the electrostatic field:^{9,10}

$$\begin{aligned} & \nabla \cdot \left[2i\omega_{pe}(D_t + \nu_e \circ) + 3v_e^2 \nabla^2 - \omega_{pe}^2 \delta N / n_0 \right] \vec{E}_1 \\ & = \frac{e}{4m_e} \nabla \cdot \left[\nabla (\vec{E}_0 \cdot \vec{E}_1^*) - \vec{E}_0 \nabla \cdot \vec{E}_1^* \right] e^{-i\Omega t} + S_E. \end{aligned} \quad (1)$$

The quantity \vec{E}_1 is the complex temporal envelope of the real electrostatic field $\vec{E} = 1/2 [\vec{E}_1(\vec{x}, t) \exp(-i\omega_{pe}t) + \text{c.c.}]$, where enveloping is carried out at the plasma frequency $\omega_{pe} = (4\pi n_0 e^2 / m_e)^{1/2}$ evaluated at the density $n_0 = 0.23 n_c$. In Eq. (1), $D_t \equiv (\partial_t + \vec{u}_0 \cdot \nabla)$ is the convective derivative for a plasma with the flow velocity \vec{u}_0 ($= 0$ here). In the absence of EM pump waves, the free solutions to Eq. (1) are LW's that propagate in a density profile whose deviation from n_0 is given by δN ($\delta N \ll n_0$). [It has been assumed that the inhomogeneity is linear ($\delta N = n_0 x / L_n$) and the direction of its gradient defines the x axis.] LW's of wave number k have the group velocity $V_g = 3k v_e^2 / \omega_{pe}$, where $v_e = \sqrt{T_e / m_e}$ is the electron thermal velocity, and their amplitudes damp at the rate $\nu_e = \nu_{\text{coll}} + \gamma_L$, which is the sum of the collisional ν_{coll} and Landau-damping

γ_L contributions. The EM field corresponding to the incident laser light is enveloped around twice ω_{pe} and further decomposed into N , coherent, linearly polarized plane waves $\vec{E}_0 = \sum_{i=1}^N \vec{E}_{0,i} \exp i(\vec{k}_{0,i} \cdot \vec{x} - \Omega_i t)$ having frequencies $\omega_{0,i}$, wave vectors $\vec{k}_{0,i}$, and vacuum intensities $I_i = c |\vec{E}_{0,i}|^2 / (8\pi)$. The quantity $\Omega_i = \omega_{0,i} - 2\omega_{pe}$ represents the mismatch for each beam, where $\max(|\Omega_i|) \ll 2\omega_{pe}$. The first term on the right-hand side of Eq. (1) is the longitudinal part of the nonlinear current, which is the origin of TPD. The term S_E is a time-random-phase Čerenkov noise source that has been described in Russell *et al.*¹⁰

A series of numerical calculations were carried out to solve Eq. (1) on a uniform $1024 \times 512 \times 512$ Cartesian grid (in the x , y , and z directions, respectively) using a 3-D generalization of the pseudospectral method that has been described previously.^{9,10} In these calculations, the electron temperature and density scale length were held constant ($T_e = 2$ keV, $L_n = 150 \mu\text{m}$), while the total overlapped intensities $I_{\text{tot}} (\equiv \sum_{i=1}^N I_i)$ was varied for various configurations of $N = 1, 2, 4$, and 6 beams of $0.351\text{-}\mu\text{m}$ -wavelength light. For each beam configuration, the single-beam intensities I_i and frequencies $\omega_{0,i}$ were taken to be equal to one another, and the beam wave vectors were distributed symmetrically to fall on the surface of a right circular cone with a 27° half-angle whose cone axis defines the x direction (see e.g., inset to Fig. 138.29). This choice of wave vectors was made because beams are distributed in well-defined cones on large laser systems such as OMEGA¹¹ and the NIF.¹² The simulation box length in the density-gradient direction (x) was chosen to include densities in the range of 0.19 to $0.27 n_c$ ($L_x = 52 \mu\text{m}$). The length in the two transverse dimensions was chosen to be $L_y = L_z = 26 \mu\text{m}$.

Figure 138.28 shows a two-dimensional (2-D) slice of the LW intensity spectrum $|E_1(\vec{k}, t)|^2$ in the $k_z = 0$ plane during the linear growth phase (averaged over times $t = 2.4$ to 4.2 ps) for a two-beam ($N = 2$) calculation. The EM wave vectors and electric-field vectors (polarization) of the two beams lie in this plane, which is the plane of maximum growth. The overlapped intensity $I_{\text{tot}} = 6 \times 10^{14} \text{ W/cm}^2$ was chosen to be above the numerically determined threshold for absolute growth. In Fig. 138.28, the bright “doublets” at the spectral locations centered on wave vectors $\vec{k} \approx (0.8, \pm 0.4, 0)k_0$ and $\vec{k} \sim (0, 0, 0)$ correspond to temporally unstable (growing) decay modes that are resonant at $n_e = 0.238 n_c$. This occurs even though each beam is individually below the threshold for absolute growth.¹³ This cooperative mode of absolutely unstable TPD is analogous to the absolutely unstable modes seen in single-beam TPD, where the pump decays into one LW with $\vec{k} \sim \vec{k}_0$

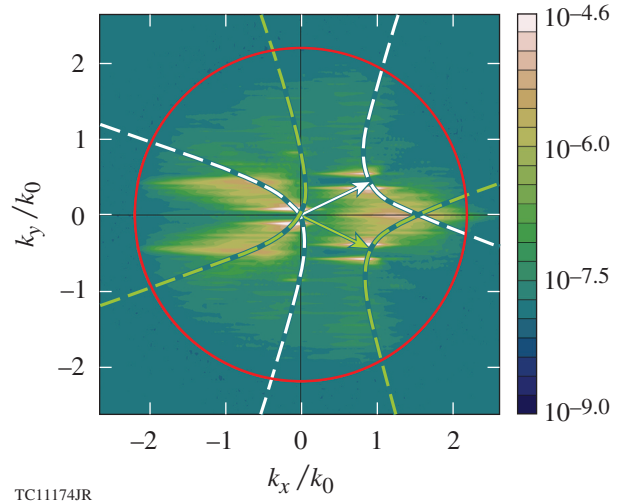
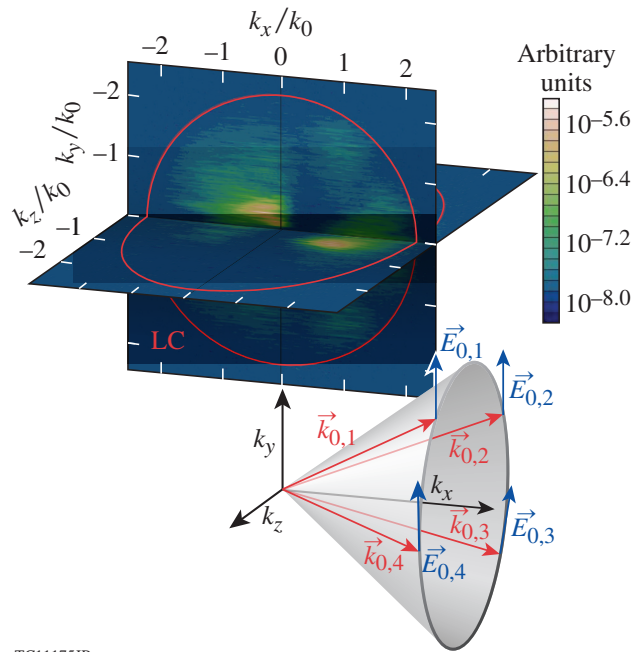


Figure 138.28

The Langmuir wave (LW) spectrum $\langle |E_1(k_x, k_y, k_z = 0, t)|^2 \rangle_t$ averaged over times $t = 2.4$ to 4.2 ps. The two electromagnetic (EM) wave vectors $\vec{k}_{0,1}$ (green arrow) and $\vec{k}_{0,2}$ (white arrow) and their polarization vectors lie in the plane shown ($k_z = 0$) (i.e., p polarization). The dashed green (white) hyperbolas correspond to the maximum single-beam homogeneous growth rate for Beam 1 (2) and the red circle is the Landau cutoff $|\vec{k}| \lambda_{De} = 0.25$ (see the text for the remaining parameters).

and another with $\vec{k} = \pm \vec{k}_\perp$, where $\vec{k}_\perp \ll \vec{k}_0$. In the two-beam case, cooperation occurs because the long-wavelength decays near $\vec{k} \approx (0, 0, 0)$ can be shared between beams. The other local maxima in $|E_1(\vec{k}, t)|^2$ located near $\vec{k} = (1.5, 0, 0)k_0$ and $\vec{k} = (-0.6, \pm 0.4, 0)k_0$ are convectively saturated (i.e., not growing) decays that are resonant at $n_e = 0.245 n_c$. These correspond to convective multibeam common waves that have been described previously^{6,14} and the “triad” modes discussed in Refs. 10, 15, and 16. The convective gain is greatest for spectral locations where the single-beam homogeneous growth-rate curves (dashed hyperbolas in Fig. 138.28) intersect [the maxima at $\vec{k} = (-0.6, \pm 0.4, 0)k_0$ correspond to the daughter waves that are not shared]. The maximum convective gain at the absolute threshold intensity has been computed numerically by estimating the enhancement of the saturated wave intensity above the steady-state noise level supported by S_E in Eq. (1). The behavior described above for two beams is quite generic. Figure 138.29 shows $|E_1(\vec{k}, t)|^2$ on the planes $k_y = 0$ and $k_z = 0$ for a four-beam calculation for the same plasma conditions as in Fig. 138.28. The beams are polarized predominantly in the y direction (signified by the symbol “ \parallel ”) as shown in the inset. The absolutely unstable modes are not restricted to a single plane. The bright spectral features near $\vec{k} = (1.0, 0 \pm 0.4)k_0$ and $\vec{k} = (-0.2, \pm 0.2, 0)k_0$ are temporally unstable and are again absolute multibeam modes. The other features in the

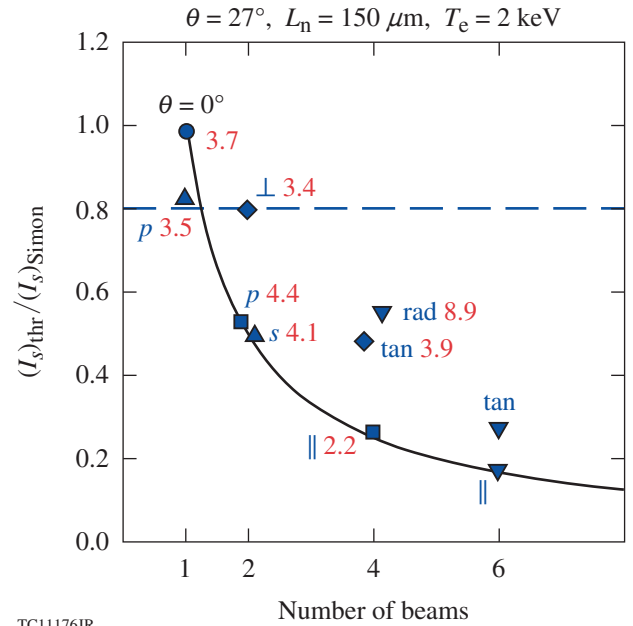


TC11175JR

Figure 138.29 Slices of the LW spectrum $\langle |E_1(\vec{k}, t)|^2 \rangle_t$ (averaged over times $t = 1.0$ to 2.0 ps) in the planes $k_y = 0$ and $k_z = 0$ for a four-beam calculation (\parallel polarization). The beam geometry and polarization are shown in the inset.

spectrum are convectively saturated. The red circles indicate the Landau cutoff.

The threshold intensity for the onset of absolute instability is found by first extracting the growth rate of the most-unstable mode, which does not saturate convectively, for a range of intensities and then finding the intensity corresponding to zero growth by extrapolation. The thresholds for collective absolute TPD instability for various configurations of $N = 1, 2, 4,$ and 6 beams are summarized in Fig. 138.30. For each configuration, there are multiple possibilities for the polarization state: “ p ” and “ s ” correspond to the one- and two-beam configurations, where the polarization is in, or out of, the plane of incidence, respectively; “ rad ” and “ tan ” refer to polarizations where the electric-field vectors are either radially or tangentially oriented with respect to the circle that forms the base of the cone containing the beam wave vectors (see inset to Fig. 138.29); the state signified as “ \parallel ” has been defined above. The thresholds have been quantified by normalizing the intensity of an individual beam for a given configuration $I_s = I_{tot}/N$ by the independent (single) beam absolute threshold given by Simon *et al.*¹³ For one beam ($N = 1$) at normal incidence ($\theta = 0^\circ$), the Simon threshold¹³ is recovered (as expected). [Notice that the threshold is lowered when the angle of incidence is increased to $\theta = 27^\circ$ (triangular marker for $N = 1$ in Fig. 138.30). The effect of



TC11176JR

Figure 138.30 Normalized single-beam threshold intensities $(I_s)_{thr}$ for absolute instability with irradiation by N beams of incidence angle $\theta_s = 27^\circ$ (except where indicated) for various polarization states (see text). The red numbers are the maximum convective gains evaluated at the absolute threshold.

oblique incidence was not described in Ref. 13 and we defer a discussion of this effect to a future publication.] The cooperative nature of the instability is revealed for $N = 2$: for both s and p polarizations, the individual (single) beam intensity at threshold $(I_s)_{thr}$ is significantly lower than the expected independent beam value (dashed line)—the importance of the effect increasing with the number of beams. Rotating the polarizations of the two beams so as to be orthogonal (“ \perp ” in Fig. 138.30) eliminates the cooperation. *The overlapping beams are parametrically unstable (absolutely) even though the threshold intensity for individual beams is not exceeded.* The solid curve indicates maximum cooperation (where the collection of beams effectively acts as a single beam with the combined intensity). The numerically estimated maximum gains of the convectively saturated common modes (cf., e.g., Fig. 138.28) at the onset of absolute instability are shown in red. These gains are consistent with earlier work.^{6,17,18} In most cases, this gain G is small ($G \lesssim 2\pi$), meaning that *the threshold for the collective absolute instability is lower than that for the convective common waves.* The regime of linear spatial amplification is therefore very restricted. Above the absolute threshold there exists a competition between the two modes of cooperative instability, which can be addressed by only a nonlinear theory.

The dominant mechanisms thought to be responsible for the nonlinear saturation of TPD [weak turbulence effects such as the Langmuir decay instability (LDI),^{8,19} profile modification,⁸ and the strong turbulence effects of cavitation and LW collapse¹⁰] are accounted for by the substitution $\delta N \rightarrow \delta N + \delta n$ in Eq. (1), where the low-frequency plasma response δn evolves according to

$$(D_t^2 + 2\nu_i \circ D_t - c_s^2 \nabla^2) \delta n = \frac{Z}{16\pi m_i} \nabla^2 \left(|\tilde{E}_1|^2 + \frac{1}{4} |\tilde{E}_0|^2 \right). \quad (2)$$

Here $c_s = (ZT_e/m_i)^{1/2} (1 + 3T_i/ZT_e)^{1/2}$ is the speed of ion-acoustic waves that damp with the rate ν_i , where m_i , T_i , and Z are the ion mass, temperature, and charge, respectively. The first term on the right-hand side describes the low-frequency ponderomotive forces of Langmuir and electromagnetic fluctuations. Together, Eq. (1), the substitution $\delta N \rightarrow \delta N + \delta n$, and Eq. (2) constitute the extended Zakharov model of TPD, previously described in Refs. 9, 10, 16, and 20, and are now generalized to three dimensions. In the context of this turbulence model where the initial ion-acoustic noise is negligible [i.e., no noise term in Eq. (2)], three regimes of cooperative TPD behavior have been identified: (1) $\tilde{I} [\equiv I_s/(I_s)_{\text{thr}}] < \tilde{I}_{\text{abs}}$ [\tilde{I}_{abs} is the threshold for collective absolute instability (Fig. 138.30)], where the LW spectrum is dominated by large- k common waves whose intensities are amplified spatially by a gain, which is numerically determined to be small $G \lesssim 3$ to 5 (red numbers in Fig. 138.30) and consistent with the standard Rosenbluth expression;⁶ (2) $\tilde{I} \gg \tilde{I}_{\text{abs}}$ —all unstable modes grow and saturate nonlinearly (the nonlinear development in this case has been described in terms of cavitating Langmuir turbulence and investigated in Ref. 16); and (3) the intermediate regime $\tilde{I} \gtrsim \tilde{I}_{\text{abs}}$. The intermediate regime is of direct relevance to spherical and planar target experiments at the Omega Laser Facility,^{6,21,22} and it displays interesting physical effects.

Figure 138.31 shows the nonlinear temporal development of the LW intensity for the two-beam p -polarized case in the intermediate regime ($\tilde{I} \gtrsim 1$) (same parameters as Fig. 138.28). The other cases shown in Fig. 138.30 exhibit very similar behavior and are not shown. The transverse (y,z) average of the LW intensity $\langle |\tilde{E}_1|^2 \rangle_{y,z}(x,t)$ is shown as a function of the x coordinate and time. At early times, growth is linear. The LW Fourier spectrum during this phase (indicated by the lower shaded region) is shown in Fig. 138.28. The previously identified absolute and convective cooperative modes occur at different spatial locations (densities), as indicated by the blue and red dashed lines, are $n_e/n_c = 0.283, 0.245$ in the figure, respectively. The blue (red) dashed vertical lines indicate the evolution of the absolute (convective) modes as a function of time (see inset). At

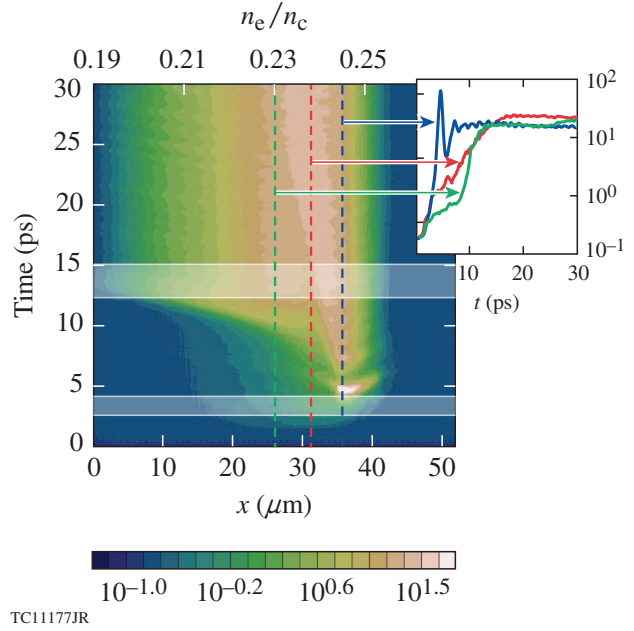
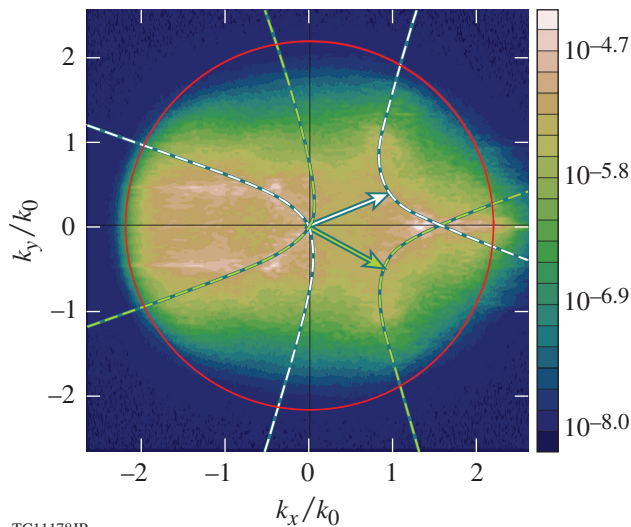


Figure 138.31

The transverse averaged LW intensity $\langle |\tilde{E}_1|^2 \rangle_{y,z}(x,t)$ as a function of the x coordinate (initial density, upper axis) and time. The inset shows the temporal dependence of $\langle |\tilde{E}_1|^2 \rangle_{\perp}(x,t)$ at the locations $x = 26 \mu\text{m}$ (dashed green line), $x = 31 \mu\text{m}$ (dashed red line), and $x = 36 \mu\text{m}$ (dashed blue line).

approximately $t = 5$ ps, the absolutely unstable modes saturate nonlinearly, producing large density-profile modifications and radiating large-amplitude LW's. These waves propagate down the density profile [toward lower densities (smaller x)] with time, generating a wave of turbulence (consistent with previous studies) whose effects can be seen in the figure. When this turbulence reaches a particular location, growth is restored to the modes that were previously convectively saturated (for $x = 26 \mu\text{m}$, this occurs at $t \sim 10$ ps). This was verified by performing a linear analysis on the perturbed profiles. The restoration of absolute growth in a convectively unstable parametric instability (i.e., fragility of the Rosenbluth result) caused by noise or turbulence has been noted previously (cf., e.g., Ref. 23). Here, it is triggered by the nonlinearity of the absolute instability. The result is that, at late times (e.g., the upper shaded region in the figure), the LW spectrum is much broader and more intense (see Fig. 138.32) than during the linear phase (Fig. 138.28). *The late-time turbulent spectrum is dominated by large- k shared (common) modes with intensities that are greatly in excess of those predicted by the linear analysis.*

These results will be of fundamental importance to direct-drive ICF experiments on the NIF, where many laser beams overlap on the target (and a knowledge of TPD stability prop-



TC11178JR

Figure 138.32

The electric-field spectrum $|E_1(\vec{k}, t)|^2$ (averaged over $t = 12$ to 15 ps) shown in the $k_z = 0$ plane for the parameters of Fig. 138.28.

erties is essential) and are an important contribution to understanding cooperative parametric instabilities in general. The results obtained with this model may provide an interpretation of experiments that infer the coexistence of large- and small-wave-number TPD LW's via half- and three-halves-harmonic emission.^{22,24} They might also explain the observation of strong TPD hot-electron production in multibeam OMEGA EP experiments, even though the predicted common-wave convective gains are small.^{6,25}

ACKNOWLEDGMENT

This material is based upon work supported by the Department of Energy National Nuclear Security Administration under Award Number DE-NA0001944, the University of Rochester, and the New York State Energy Research and Development Authority. The support of DOE does not constitute an endorsement by DOE of the views expressed in this article.

REFERENCES

1. J. Nuckolls *et al.*, *Nature* **239**, 139 (1972).
2. J. D. Lindl, *Inertial Confinement Fusion: The Quest for Ignition and Energy Gain Using Indirect Drive* (Springer-Verlag, New York, 1998).
3. R. P. Drake, *High-Energy-Density Physics: Fundamentals, Inertial Fusion, and Experimental Astrophysics*, Shock Wave and High Pressure Phenomena (Springer, Berlin, 2006).
4. D. F. DuBois *et al.*, *Phys. Plasmas* **8**, 791 (2001); P. Y. Cheung *et al.*, *Phys. Plasmas* **8**, 802 (2001).
5. M. J. Edwards, P. K. Patel, J. D. Lindl, L. J. Atherton, S. H. Glenzer, S. W. Haan, J. D. Kilkenny, O. L. Landen, E. I. Moses, A. Nikroo, R. Petrasso, T. C. Sangster, P. T. Springer, S. Batha, R. Benedetti, L. Bernstein, R. Betti, D. L. Bleuel, T. R. Boehly, D. K. Bradley, J. A. Caggiano, D. A. Callahan, P. M. Celliers, C. J. Cerjan, K. C. Chen, D. S. Clark, G. W. Collins, E. L. Dewald, L. Divol, S. Dixit, T. Doeppner, D. H. Edgell, J. E. Fair, M. Farrell, R. J. Fortner, J. Frenje, M. G. Gatu Johnson, E. Giraldez, V. Yu. Glebov, G. Grim, B. A. Hammel, A. V. Hamza, D. R. Harding, S. P. Hatchett, N. Hein, H. W. Herrmann, D. Hicks, D. E. Hinkel, M. Hoppe, W. W. Hsing, N. Izumi, B. Jacoby, O. S. Jones, D. Kalantar, R. Kauffman, J. L. Kline, J. P. Knauer, J. A. Koch, B. J. Kozioziemski, G. Kyrala, K. N. LaFortune, S. Le Pape, R. J. Leeper, R. Lerche, T. Ma, B. J. MacGowan, A. J. MacKinnon, A. Macphee, E. R. Mapoles, M. M. Marinak, M. Mauldin, P. W. McKenty, M. Meezan, P. A. Michel, J. Milovich, J. D. Moody, M. Moran, D. H. Munro, C. L. Olson, K. Opachich, A. E. Pak, T. Parham, H.-S. Park, J. E. Ralph, S. P. Regan, B. Remington, H. Rinderknecht, H. F. Robey, M. Rosen, S. Ross, J. D. Salmonson, J. Sater, D. H. Schneider, F. H. Séguin, S. M. Sepke, D. A. Shaughnessy, V. A. Smalyuk, B. K. Spears, C. Stoeckl, W. Stoeffl, L. Suter, C. A. Thomas, R. Tommasini, R. P. Town, S. V. Weber, P. J. Wegner, K. Widman, M. Wilke, D. C. Wilson, C. B. Yeaman and A. Zylstra, *Phys. Plasmas* **20**, 070501 (2013).
6. D. T. Michel, A. V. Maximov, R. W. Short, S. X. Hu, J. F. Myatt, W. Seka, A. A. Solodov, B. Yaakobi, and D. H. Froula, *Phys. Rev. Lett.* **109**, 155007 (2012).
7. V. A. Smalyuk, D. Shvarts, R. Betti, J. A. Delettrez, D. H. Edgell, V. Yu. Glebov, V. N. Goncharov, R. L. McCrory, D. D. Meyerhofer, P. B. Radha, S. P. Regan, T. C. Sangster, W. Seka, S. Skupsky, C. Stoeckl, B. Yaakobi, J. A. Frenje, C. K. Li, R. D. Petrasso, and F. H. Séguin, *Phys. Rev. Lett.* **100**, 185005 (2008); V. N. Goncharov, T. C. Sangster, P. B. Radha, R. Betti, T. R. Boehly, T. J. B. Collins, R. S. Craxton, J. A. Delettrez, R. Epstein, V. Yu. Glebov, S. X. Hu, I. V. Igumenshchev, J. P. Knauer, S. J. Loucks, J. A. Marozas, F. J. Marshall, R. L. McCrory, P. W. McKenty, D. D. Meyerhofer, S. P. Regan, W. Seka, S. Skupsky, V. A. Smalyuk, J. M. Soures, C. Stoeckl, D. Shvarts, J. A. Frenje, R. D. Petrasso, C. K. Li, F. Séguin, W. Manheimer, and D. G. Colombant, *Phys. Plasmas* **15**, 056310 (2008).
8. H. X. Vu, D. F. DuBois, J. F. Myatt, and D. A. Russell, *Phys. Plasmas* **19**, 102703 (2012).
9. D. F. DuBois, D. A. Russell, and H. A. Rose, *Phys. Rev. Lett.* **74**, 3983 (1995).
10. D. A. Russell and D. F. DuBois, *Phys. Rev. Lett.* **86**, 428 (2001).
11. T. R. Boehly, D. L. Brown, R. S. Craxton, R. L. Keck, J. P. Knauer, J. H. Kelly, T. J. Kessler, S. A. Kumpan, S. J. Loucks, S. A. Letzring, F. J. Marshall, R. L. McCrory, S. F. B. Morse, W. Seka, J. M. Soures, and C. P. Verdon, *Opt. Commun.* **133**, 495 (1997).
12. E. I. Moses *et al.*, *Phys. Plasmas* **16**, 041006 (2009); E. I. Moses, *Fusion Sci. Technol.* **54**, 361 (2008); W. J. Hogan, E. I. Moses, B. E. Warner, M. S. Sorem, and J. M. Soures, *Nucl. Fusion* **41**, 567 (2001); J. A. Paisner, E. M. Campbell, and W. J. Hogan, *Fusion Technol.* **26**, 755 (1994).
13. A. Simon, R. W. Short, E. A. Williams, and T. Dewandre, *Phys. Fluids* **26**, 3107 (1983).
14. D. T. Michel, A. V. Maximov, R. W. Short, J. A. Delettrez, D. Edgell, S. X. Hu, I. V. Igumenshchev, J. F. Myatt, A. A. Solodov, C. Stoeckl, B. Yaakobi, and D. H. Froula, *Phys. Plasmas* **20**, 055703 (2013).

15. H. X. Vu, D. F. DuBois, D. A. Russell, and J. F. Myatt, *Phys. Plasmas* **19**, 102708 (2012).
16. H. X. Vu, D. F. DuBois, D. A. Russell, J. F. Myatt, and J. Zhang, "Nonlinear Development of the Two-Plasmon Decay Instability in Three Dimensions," to be published in *Physics of Plasmas*.
17. R. Yan, A. V. Maximov, and C. Ren, *Phys. Plasmas* **17**, 052701 (2010).
18. M. N. Rosenbluth, *Phys. Rev. Lett.* **29**, 565 (1972).
19. D. F. DuBois and M. V. Goldman, *Phys. Rev.* **164**, 207 (1967).
20. J. F. Myatt, H. X. Vu, D. F. DuBois, D. A. Russell, J. Zhang, R. W. Short, and A. V. Maximov, *Phys. Plasmas* **20**, 052705 (2013).
21. C. Stoeckl, R. E. Bahr, B. Yaakobi, W. Seka, S. P. Regan, R. S. Craxton, J. A. Delettrez, R. W. Short, J. Myatt, A. V. Maximov, and H. Baldis, *Phys. Rev. Lett.* **90**, 235002 (2003).
22. W. Seka, D. H. Edgell, J. F. Myatt, A. V. Maximov, R. W. Short, V. N. Goncharov, and H. A. Baldis, *Phys. Plasmas* **16**, 052701 (2009).
23. D. R. Nicholson and A. N. Kaufman, *Phys. Rev. Lett.* **33**, 1207 (1974); G. Laval, R. Pellat, and D. Pesme, *Phys. Rev. Lett.* **36**, 192 (1976); E. A. Williams, J. R. Albritton, and M. N. Rosenbluth, *Phys. Fluids* **22**, 139 (1979).
24. W. Seka, J. F. Myatt, R. W. Short, D. H. Froula, J. Katz, V. N. Goncharov, and I. V. Igumenshchev, "Nonuniformly Driven Two-Plasmon-Decay Instability in Direct-Drive Implosions," to be published in *Physical Review Letters*.
25. P. Michel *et al.*, *Phys. Plasmas* **20**, 056308 (2013).